

# A DUAL KLYSTRON SOLID-STATE MODULATOR FOR THE TERA-LIBO 30 MEDICAL ACCELERATOR SYSTEM

P. Pearce, TERA Foundation, Novara, Italy  
 L. Shen, IHEP, Beijing, P.R. China

## Abstract

The LIBO medical accelerator project of the TERA Foundation will use a commercially available 30 MeV cyclotron as an injector to a compact linear accelerator to provide a 200 MeV proton beam for cancer therapy treatment of deep-seated tumours. This arrangement will enable a range of beam energies for proton therapy while the cyclotron can continue to produce radioisotopes for related cancer diagnostic procedures. Equipment space requirements, operational reliability, availability and maintainability as well as costs are major factors to be considered in the design of a hospital medical facility. Compact solid-state modulators, each capable of driving two medical S-band klystrons and operating at 200Hz repetition frequency with a pulse width of 5 $\mu$ s, have been designed for this linac application. This paper describes the layout of the RF system and the design of the dual klystron solid-state modulators (DKSSM) to be used, and compares the simulated results to the LIBO 30 requirements.

## THE LIBO SYSTEM

The Linac Booster (LIBO) is a 3 GHz high gradient (17-19 MV/m) proton accelerator that uses a 30 MeV cyclotron as its injector. This compact side-coupled linac (about 16 m in length) boosts the energy of the protons from the cyclotron up to the maximum 210 MeV level. A full prototype accelerating module has already been designed, constructed and tested [1] at CERN, Geneva, Switzerland and then tested with a cyclotron beam at the Laboratori Nazionali del Sud of INFN in Catania, Italy.

The LIBO 30 main parameters are given in Table 1. The general scheme of the RF system with the dual klystron modulators connected to accelerating modules (two half-modules), are shown in Figure 1. Each klystron is driven by solid-state RF amplifiers (~100 watts) and each have an adjustable low-level phase controller incorporated.

Table 1: LIBO 30 Main Parameters

Parameter	Value
Accelerating RF frequency	2998.5 MHz
Number of accelerating modules	10
Number of tanks per half module	2
Number of accelerating cells per tank	14
Number of klystrons	20
Number of dual klystron-modulators	10
Active linac length	16.4 m
Axial accelerating field on axis	17-19 MV/m
Total peak RF power required for linac	60.8 MW
Duty cycle (200 Hz and 5 $\mu$ s pulse width)	~0.1%
Average RF power required for the linac	~60.8 kW

All LIBO modules are essentially identical, except for their gradual increase in length that corresponds to the increasing velocity of the protons down the linac. Each half module has 28 accelerating cells configured as two tanks driven by one klystron from a dual klystron solid-state modulator. The two tanks in the half module are resonantly connected with a bridge-coupler that serves also as the RF input power feeder point. Permanent magnet quadrupoles (160-130 T/m) are located in the two end-cells of each half module as well as in the bridge-coupler, forming a FODO focusing lattice. The RF peak power, energy gain and accelerating gradient for each complete pair of accelerating modules [2] are in Table 2.

Table 2: LIBO 30 Modules RF Power requirements

Half-module pairs M (n,m)	Voltage gradient MV/m	Full Module energy gain MeV	Half-module-(n) peak RF power MW	Half-module-(m) peak RF power MW
1,2	17	10.14	3.042	3.049
3,4	18	12.24	3.035	3.044
5,6	19	14.24	3.03	3.042
7,8	19	16.14	3.041	3.046
9,10	19	17.89	3.045	3.048
11,12	19	19.48	3.051	3.048
13,14	19	20.84	3.041	3.047
15,16	19	22.11	3.05	3.049
17,18	19	23.21	3.04	3.046
19,20	19	24.22	3.047	3.052

## THE DKSSM SYSTEM

There are ten identical dual klystron solid-state modulators in the total LIBO 30 system. Each klystron output can be adjusted to produce 4 MW of peak RF power, although operationally only about 3.5 MW would be needed. The S-band klystrons have a nominal microperveance of 2.0 and an electronic efficiency of about 41%. Focusing of the electron beam in the klystron is done with a single water-cooled magnet coil requiring about 5 kW dc power.

The basic electrical circuit of the solid-state modulator is given in Figure 2. A storage capacitor is charged to about 10kV from a switched-mode power supply and then discharged with a solid-state switch [3] into the primary of a step-up pulse transformer.

An Integrated Gate Commutated Thyristor (IGCT) high-voltage switch assembly, shown in Figure 3, is used to discharge the capacitor. The IGCT assembly has four (4.5 kV, 4 kA) devices in series that are asymmetric blocking types [4] with fast turn-on and turn-off times and low switching and on-state losses. A simple

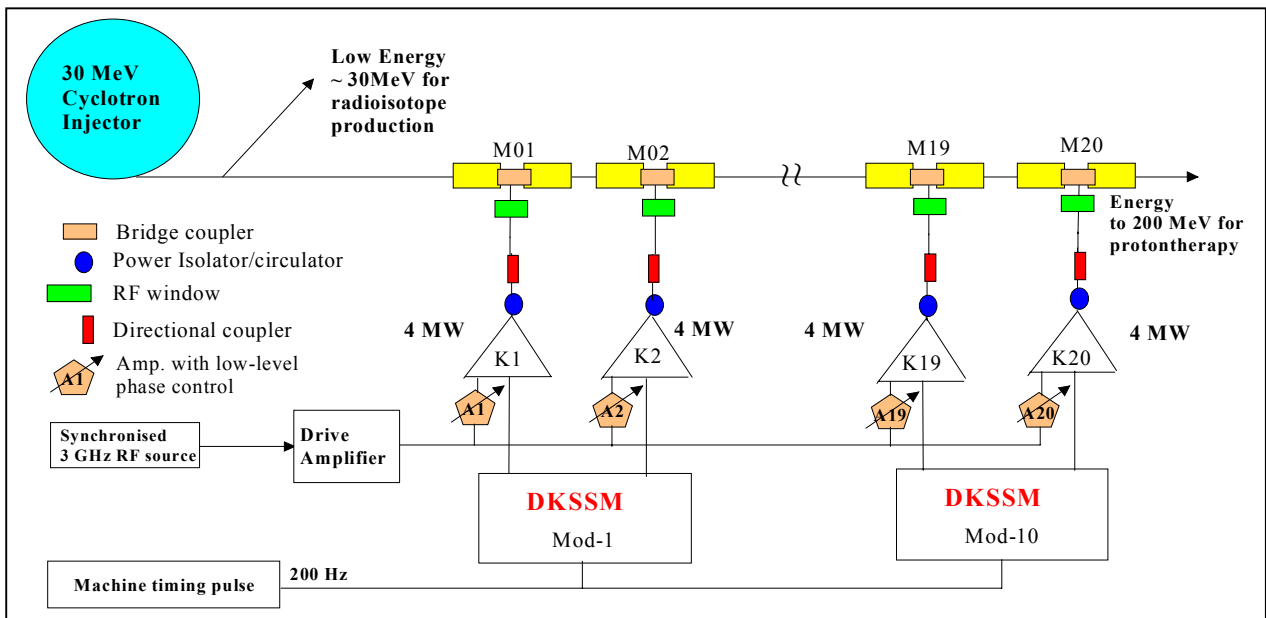


Figure 1: The LIBO RF and Dual Klystron-Modulator Scheme

optical-fibre control interface with status feedback from each device is used to trigger the switch assembly. The IGCT combines the advantages of the GTO thyristor and the IGBT (Insulated Gate Bipolar Transistor), but unlike an IGBT at turn-off, the IGCT gate is reversed biased to absorb the anode current. This hard turn-off mode of operation is made possible by on-chip optically coupled gate drivers that reduce the carrier storage time to about 1 $\mu$ s. This also enables easier series stacking of the devices without close parameter selection.

pulse on the cathodes of the parallel-connected grounded anode klystrons. The modulator high-voltage pulse width is determined by the width of the IGCT optical trigger pulse giving full pulse width flexibility. The matching network inductance L1 has in parallel a diode and resistor circuit (D1, R1) that helps to clamp the IGCT anode voltage, at turn-off, to the voltage level on the storage capacitors.

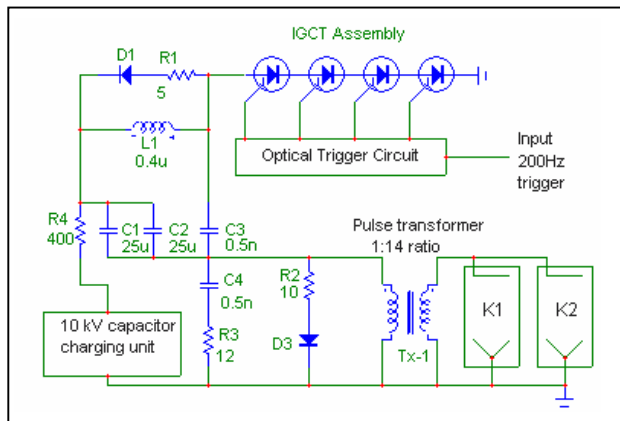


Figure 2: Basic electric circuit of a DKSSM

The 91 mm diameter devices are encapsulated in low inductance housings and the operating voltage across each series device is derated by about 30% to improve reliability and avoid false triggering due to cosmic radiation. Each IGCT device is cooled with de-ionized water having a flow rate of 4 litres per minute.

In operation, when the IGCT assembly is triggered ON the positive terminals of the storage capacitors C1 and C2 are grounded. The opposite terminals swing the pulse transformer negative creating a high-voltage negative



Figure 3: IGCT assembly

The high-voltage pulse transformer has a step-up ratio of 1:14 and has a strip wound steel core. In order to provide separate heater power control for each of the two klystrons, the transformer has bifilar secondary windings on each leg of the core. A dc core bias of about 15 A is required on the primary winding to prevent transformer core saturation, and the low voltage power unit that provides this bias current is isolated with a 20 mH inductor. The maximum secondary winding voltage is about 140 kV, and under normal operation at 4 MW peak output power from each klystron, the peak secondary

voltage and current is about 120 kV and 165 A. The transformer leakage inductance and stray capacitance, including that of the two klystrons, are included in the calculation of the klystrons pulse voltage rise and fall times (10 to 90%). The dual klystron solid-state modulator parameters are given in Table 3 below.

Table 3: DKSSM parameters

Parameter	Value	Units
Klystron peak RF output	4	MW
Klystron voltage	119	kV
Klystron current	82	A
RF pulse width	5	μs
Voltage pulse width FWHM	7.8	μs
Repetition frequency	200	Hz
Klystron efficiency	41	%
Klystron perveance	2.0	A/V <sup>1.5</sup>
Voltage pulse energy	142	J
Capacitor charging voltage	8.65	kV
IGCT switch peak current	2300	A
Capacitor recharging power	38	kW
Pulse transformer ratio	1:14	-

Two low inductance storage capacitors C1 and C2 are in parallel to reduce the total inductance of the energy source and also to share the primary circuit discharge current of about 2300 A. To reduce any positive voltage excursions on the cathodes of the klystrons, a diode and resistor clamp (D3, R2) is placed directly across the primary winding of the pulse transformer. Carbon disc ceramic resistors are used in the modulator design for all low ohmic value power resistors.

A 40 kW switch-mode high-voltage (10 kV) capacitor charging power unit is to be used for the recharging cycle of the storage capacitors as shown in Figure 4. Since the

energy stored in these capacitors is relatively high compared to the pulse energy used, the delta voltage recovery after each pulse is small.

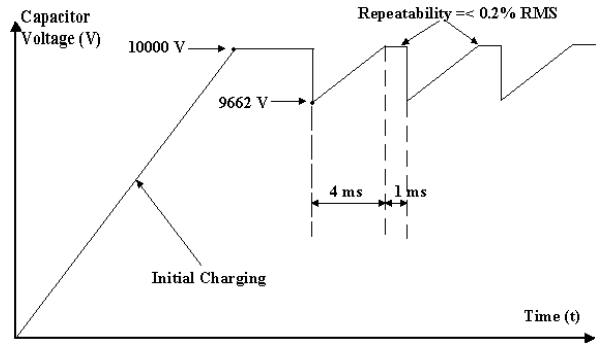


Figure 4: Storage capacitor charge and discharge cycle

A flat top period of about 1ms is left for stabilisation of the voltage level after each pulse. The power unit acts as a constant current source until the reference voltage is reached, and the unit goes into voltage regulation mode. Resistor R4 is used to isolate the capacitor load from the power unit and reduces the capacitor discharge current back into the power unit in the case of a fault. Voltage repeatability should be around 0.2% RMS at full voltage.

### DKSSM CIRCUIT SIMULATION

Simulation of the DKSSM has been mostly made using MicroCap V6 [5] using the circuit of Figure 5. The IGCT assembly was modeled using ideal ON-OFF switches together with the RC snubber components, a voltage dependent function for the four MOV resistors, and a high-voltage diode model for the protection diodes D4 to D7. Measured stray circuit capacitances are C9 to C12.

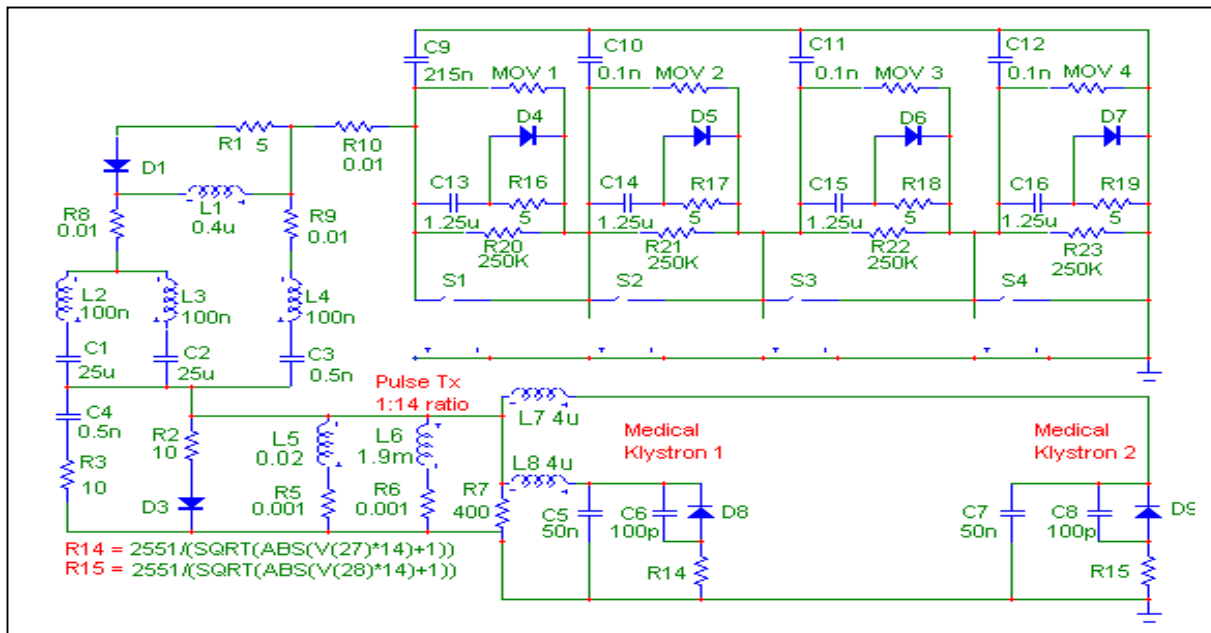


Figure 5: DKSSM Simulation circuit

The IGCT assembly is made by ABB, Switzerland. For ease of simulation all components on the secondary windings have been referred to the primary side of the pulse transformer. The two klystron amplifiers are modeled by writing their referred dynamic impedance (see Eq. 1) as a function of the turns ratio (N) squared, the micro-perveance and the square root of the node voltage (Vx) at the point where these non-linear resistors R14 and R15 are located.

$$R'_K = \frac{1}{N^2 \mu P \sqrt{V_x}} \quad (1)$$

The pulse transformer turns ratio was optimised with respect to the IGCT parameters in Table 4, to keep the voltages across individual devices inside the 30% safety margin, and the peak current and di/dt inside the maximum ratings.

Table 4: IGCT switch assembly parameters

Parameter	Value	Units
Forward peak off-state voltage	4500	V
Reverse peak off state voltage	4500	V
On-state voltage across assembly	≤ 31	V
Maximum On-state current	4000	A
Maximum current rate-of-rise	3000	A/μs
Turn-On trigger energy	≤ 1.5	J
Turn-On delay time	< 3	μs
Maximum controlled turn-off current	4000	A
Turn-Off trigger energy	19.5	J
Turn-Off time delay	< 6	μs

The circuit design stability was verified by calculating the IGCT voltages and currents over a projected klystron lifetime of 30,000 hours, for a 20% variation in micro-perveance, at a constant 4 MW output power. The range of charging voltage and switch current at 4 MW output from each klystron, versus changes in micro-perveance are shown in Figure 6.

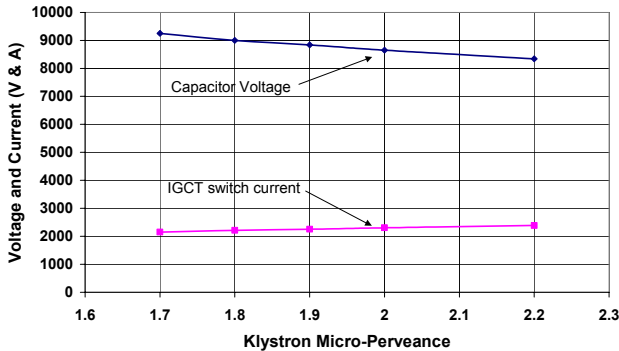


Figure 6: Voltage and IGCT current vs Micro-perveance

The storage capacitor values have been optimised for getting an acceptable 1% voltage droop over the 5 μs flat top of the pulse. The voltage droop curve of Figure 7 was obtained from simulations in MicroCap. The rise and fall

times of the simulated voltage pulse are 1.3 μs and 1.7 μs respectively. The simulated voltage pulse width at FWHM was found to be about 8 μs.

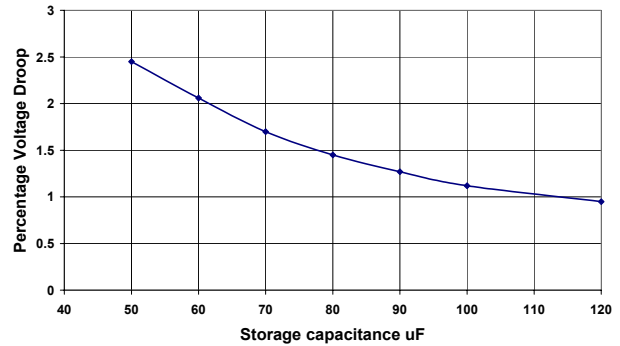


Figure 7: Flat top droop vs storage capacitance

The main pulse transformer components [6] shown in Figure 5 are the primary inductance L6, the core-loss resistance R7 while L7 and L8 are the total leakage inductance values attributed to the two secondary bifilar windings. The each stray secondary winding capacitance summed with the klystron capacitance are represented by C5 and C7. The klystrons [7] are modeled with the non-linear resistor functions for R14 and R15 together with the high-voltage diodes D8 and D9.

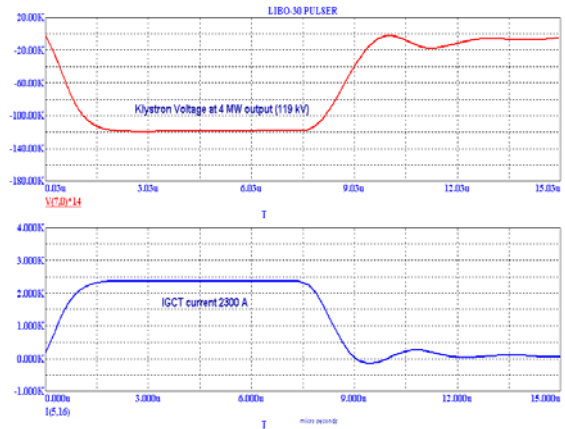


Figure 8: Simulated voltage and current waveforms

Figure 8 shows the simulated high voltage that is applied separately to both klystrons from each secondary bifilar winding. The longer voltage fall time is due mainly to the stored energy in the transformer magnetizing inductance after the IGCT assembly has been switched off as seen above. The core loss resistance (non-linear) and the low value snubber resistors (across each IGCT device) are effectively in parallel affecting the L/R time constant during the recovery of the pulse transformer.

In the final construction, the klystron tank and pulse transformer may be connected to the modulator via a low impedance coaxial cable. The impedance mismatch can cause oscillations during the rise of the voltage pulse and the filter C4, R3, included in the simulation circuit, will be used to dampen these out.

## OPERATION AND PROTECTION

The RF phase adjustment of each klystron will be made at the low level RF input. The 100-watt peak output, solid-state driver-amplifiers, will have incorporated an electronic phase shifter as shown in Figure 1. All of the ten modulators will be synchronized with a 200 Hz machine pulse.

The output power of any two klystrons driven from a single DKSSM will be the same since they both receive the same voltage pulse. Each klystrons power can however be adjusted individually (reduced) by small amounts (up to about 5%) by reducing the RF drive level to the klystron. Varying the input RF drive voltage changes the klystron bunching parameter, which affects the beam current, and therefore the output power, by taking the klystron out of saturated operating mode. A power isolator at the exit of each klystron will protect it for excessive reflected power. Bi-directional RF couplers are located in each output waveguide circuit for detecting both forward and reflected power levels and to be used for protection and measurement purposes.

Protection of solid-state switches in pulsed circuits is an issue that has to be addressed early in the design of the modulator. The DC voltage distribution across the four IGCT devices is made with resistors R20 to 23, and RC snubber circuits and diodes handle the AC and pulsed voltage conditions. The Metal Oxide Varistors (MOV) will reduce the amplitude of fast voltage transients from high-voltage breakdowns in the klystron gun regions.

The detection of gun breakdowns, by monitoring the klystrons vacuum ion-pump current is a very sensitive interlock to such events. The peak level of IGCT current can be detected with a current transformer and also used as an interlock. These two signals can be used to switch off the IGCT to avoid damage to the device for repeated fault conditions. Figure 9 shows the increasing IGCT current for a simulated klystron gun short circuit fault condition lasting 200ns during the rise time of the pulse.

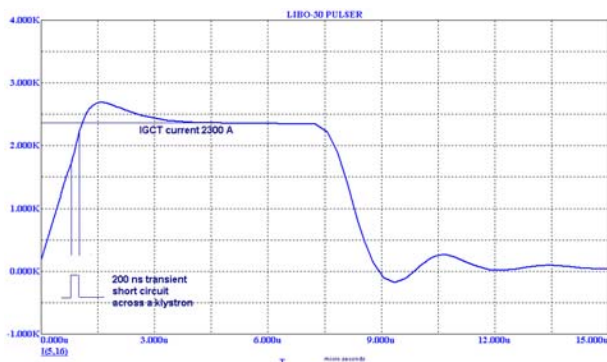


Figure 9: IGCT current under fault conditions

Additionally, the high-voltage on the storage capacitors is monitored and compared to the preset maximum reference voltage. If this level is exceeded at any time the charging unit would be switched off.

## SUMMARY

The calculations and simulations made with the dual klystron solid-state modulator equivalent circuit show that a compact and simple pulsed RF system can be made with an IGCT switching device. Additional experience [3] with a similar solid-state modulator driving one klystron, at a lower voltage level and at 100 Hz rate has already been made. The simulated waveforms together with previous test modulator results show that the pulse performance needed for the LIBO-30 system can be obtained. Although no solid-state IGCT switches have been damaged in the previous tests, it is realized that protection and control of these pulsed systems is an important design issue. A DKSSM system for LIBO-30 should be constructed and tested in the very near future.

## ACKNOWLEDGEMENTS

The authors would like to acknowledge the help and encouragement of Professor Ugo Amaldi of the TERA Foundation in this work, and the detailed discussions on the accelerating cavity module design with Drs Mario Weiss and Riccardo Zennaro also from the TERA Foundation.

## REFERENCES

- [1] U. Amaldi et al., "LIBO-a linac-booster for proton therapy: construction and tests of a prototype," Nuclear Instruments and Methods in Physics Research A, NIMA.42238 (2003).
- [2] R. Zennaro, private communication.
- [3] P. Pearce et al., "A 50 Hz Low-Power Solid-State Klystron-Modulator," IEE European Pulsed Power Symposium, French German Research Institute, Saint-Louis, France, October 2002.
- [4] ABB Semiconductors Switzerland, "Specification for Reverse Blocking IGCT switch Type A-SBP 35L45-4-WC-PS," 2003
- [5] Micro-Cap 6, Spectrum Software, Sunnyvale, CA, USA, 1999.
- [6] Stangenes Industries, Palo Alto, CA, USA, 2003.
- [7] CPI Klystrons, Stanford, CA, USA, 2003.